DYNAMIC MAGMATIC PROCESSES RECORDED IN THE TULAMEEN ULTRAMAFIC-MAFIC ALASKAN-TYPE INTRUSION FROM OUTCROP-SCALE STRUCTURES AND MINERAL-SCALE TEXTURES

Dylan W. Spence[1,a], James S. Scoates[1], Ian R. Goan[1], James A. Nott[1], Graham T. Nixon[2], and Dejan Milidragovic[3,1]

[1]Pacific Centre for Isotopic and Geochemical Research, [2]British Columbia Geological Survey, [3]Geological Survey of Canada

[a]dspence@eoas.ubc.ca

ABSTRACT

The Late Triassic Tulameen intrusion, located in the southern Quesnel terrane, is the largest exposed Alaskan-type ultramafic-mafic intrusion in the North American Cordillera. It is zoned outward from a dunite core to olivine clinopyroxenite and hornblende clinopyroxenite, and also contains widespread gabbroic to syenitic phases. Fieldwork (2021, 2022, 2023) has revealed that the Tulameen intrusion displays complex magmatic structures and textures at the macroscopic (outcrop) and microscopic (thin section) scales. Outcrop-scale mapping has been facilitated through acquisition of high-quality imagery using remotely piloted aircraft system (RPAS) photogrammetry and by mobile-device light detection and ranging (LiDAR) to produce 3D digital models of individual outcrops. Within the olivine-bearing units, magmatic structures include dikes and veins of clinopyroxenite within dunite, and dike-like bodies and irregular disaggregated enclaves of dunite to wehrlite within olivine clinopyroxenite. Clinopyroxene- and hornblende-bearing units display discontinuous layering and laminations of hornblende and magnetitite, and pegmatitic segregations of hornblende are common. Hornblende clinopyroxenite and hornblendite, as well as feldspar-bearing gabbroic to syenitic units, consistently show intermingled contact relationships with highly variable textures. At the grain scale, mineral textures are notably heterogeneous. Olivine crystals range from tabular to megacrystic and are locally intensely kink-banded. Clinopyroxenites are commonly inequigranular displaying interdigitated grain boundary relationships. Hornblende replaces clinopyroxene and forms mineral laminations and discontinuous veins. The diversity of magmatic structures and mineralogical textures documented in the Tulameen Alaskan-type intrusion is consistent with emplacement as part of a physically and chemically dynamic and open magmatic system dominated by mingling between crystal-rich magmas.

ALASKAN-TYPE INTRUSIONS

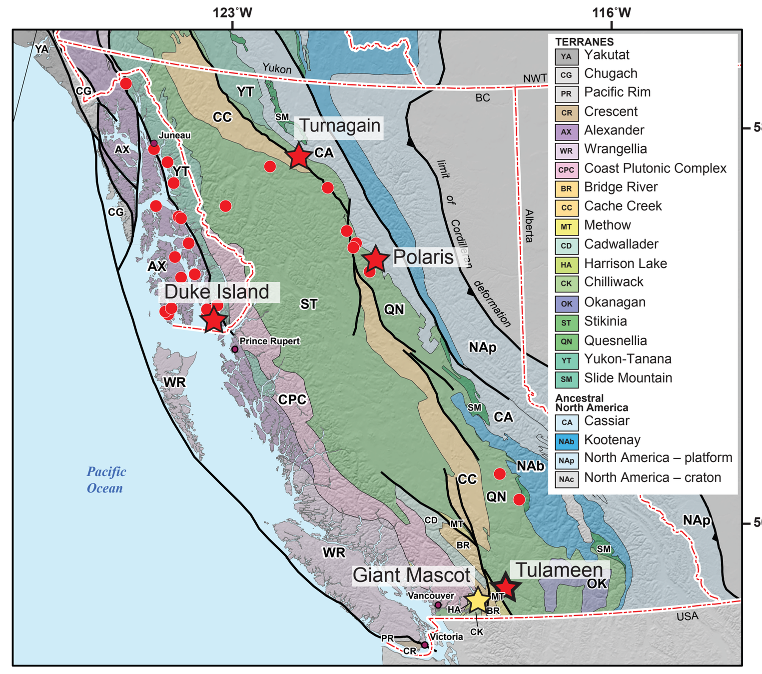

Alaskan-type intrusions are convergent margin ultramafic-mafic intrusions that are characteristically devoid of orthopyroxene. Alaskan-type intrusions are commonly associated with **Cr-Ni-Cu-Au-PGE mineralization**.

LEFT: Locations of ultramafic-mafic Alaskan-type intrusions (red) (after Himmelberg and Loney, 1995; Nixon et al., 1997) including the Tulameen intrusion (bold), the orthopyroxene-bearing Giant Mascot intrusion (yellow) (Manor et al., 2016) and terranes of the North American Cordillera (modified from Colpron and Nelson, 2011). Major intrusions are marked with a star.

BOTTOM: IUGS ternary classification of ultramafic rocks (Le Maitre, 1989) with unofficial sub-classifications of olivine wehrlite and wehrlite and modal analyses for typical ultramafic rocks in the Tulameen intrusion illustrating the characteristic lack of orthopyroxene in Alaskan-type intrusions (adapted from Nixon et al., 2015). Representative hand-sample photographs of selected rock types including syenite. Feldspar-bearing rock-types range from monzogabbro to syenite and are present on the eastern margin of the Tulameen intrusion (see next section).

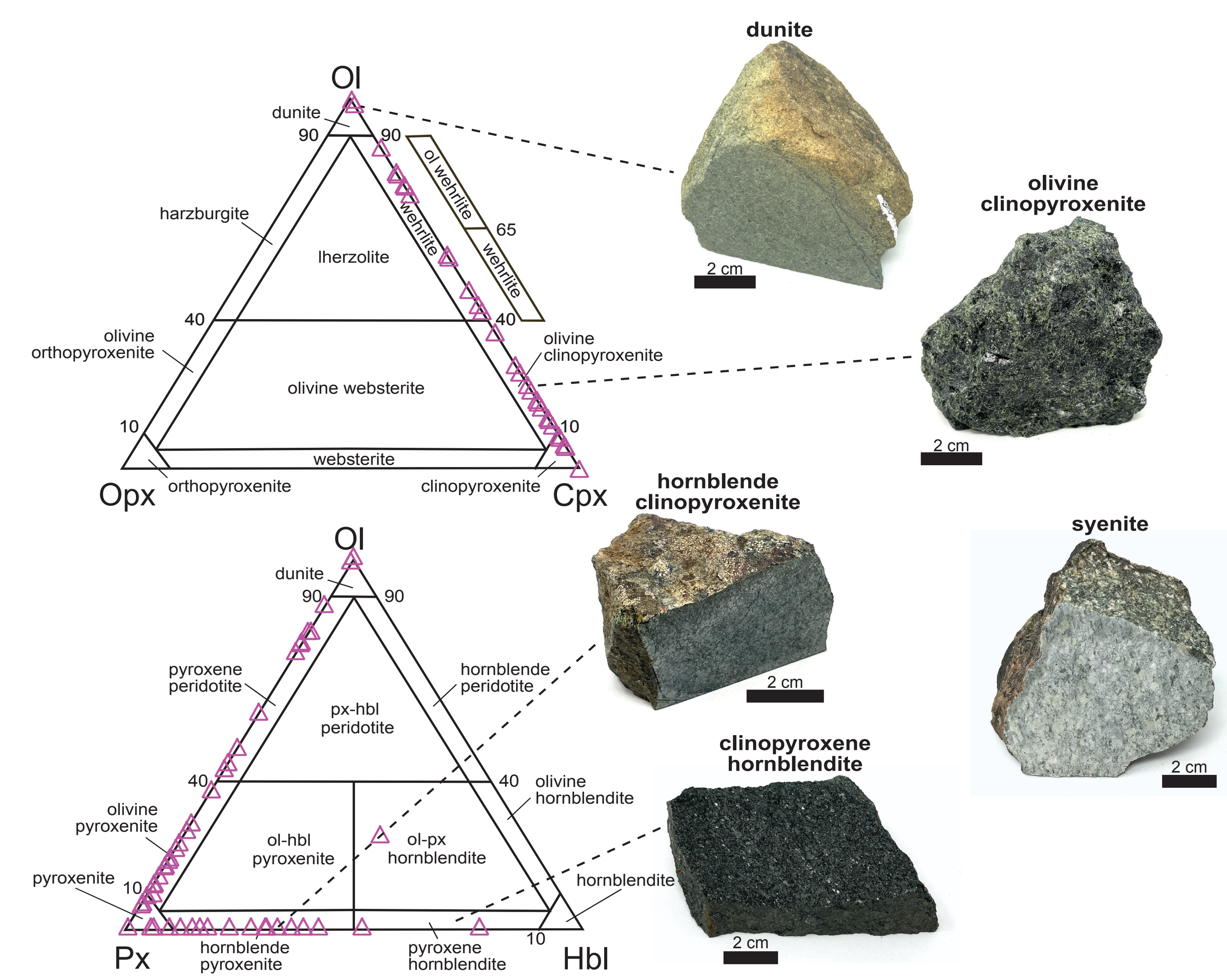

MAGMATIC STRUCTURES

CLINOPYROXENITE DIKES

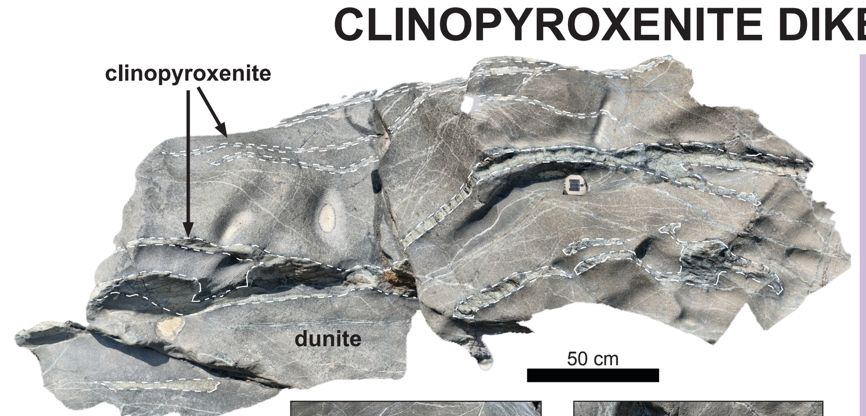

Steps for viewing augmented reality (AR) models on iPhone:
1. Scan QR code
2. Select/download file with extension .usdz and open
3. View model in "AR" for to-scale model projected on floor, or select "Object" to view model on phone screen

TOP: 3D LiDAR model of dunite with discontinuous and anastamosing clinopyroxenite dikes ranging from tabular in shape to undulating (outlined with dashed line).

BOTTOM LEFT: Photograph of discontinuous tabular clinopyroxenite dikes (outlined with dashed line) within dunite. Scratcher (13 cm) for scale.

BOTTOM RIGHT: Close-up photograph of clinopyroxenite dikes (outlined with dashed line) within dunite. One of the dikes is discontinuous; it is difficult to discern if the dikes resulted from the same magmatic event or if they are cross-cutting. Scratcher for scale.

DUNITE AND WEHRLITE ENCLAVES

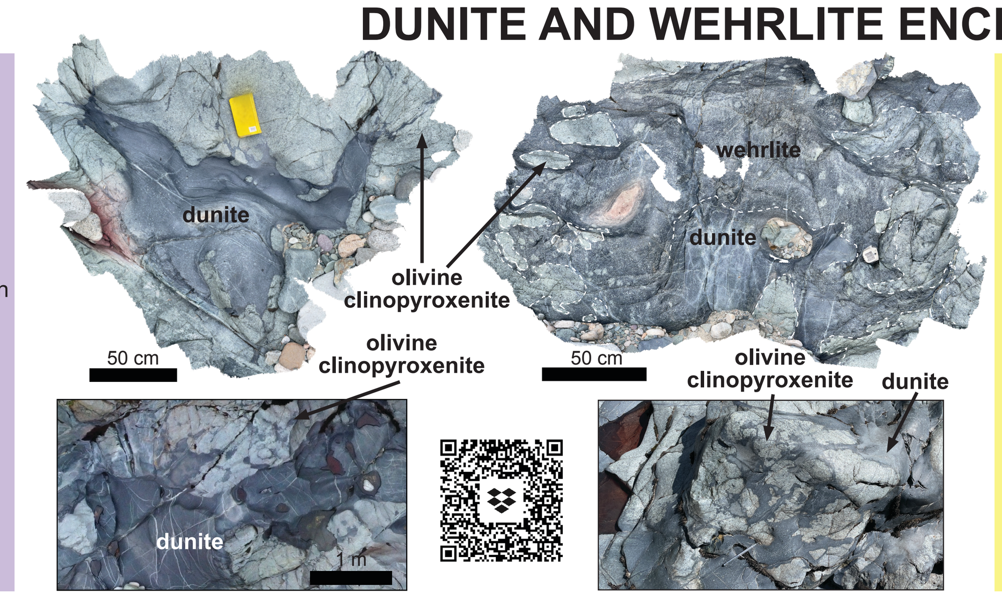

TOP LEFT: 3D LiDAR model of dunite enclave within olivine clinopyroxenite with sharp contacts and tips.

TOP RIGHT: 3D LiDAR model of dunite to wehrlite enclave within olivine clinopyroxenite. Olivine clinopyroxenite enclaves are also contained within the wehrlite. Contacts between dunite and wehrlite range from sharp to diffuse. Selected contacts are illustrated with dashed line.

BOTTOM LEFT: Snapshot from RPAS orthomosaic of dunite enclave within olivine clinopyroxenite with irregular protrusions.

BOTTOM RIGHT: Photograph of anastamosing dike-like bodies of dunite originating from larger enclaves of dunite within olivine clinopyroxenite. Scratcher for scale.

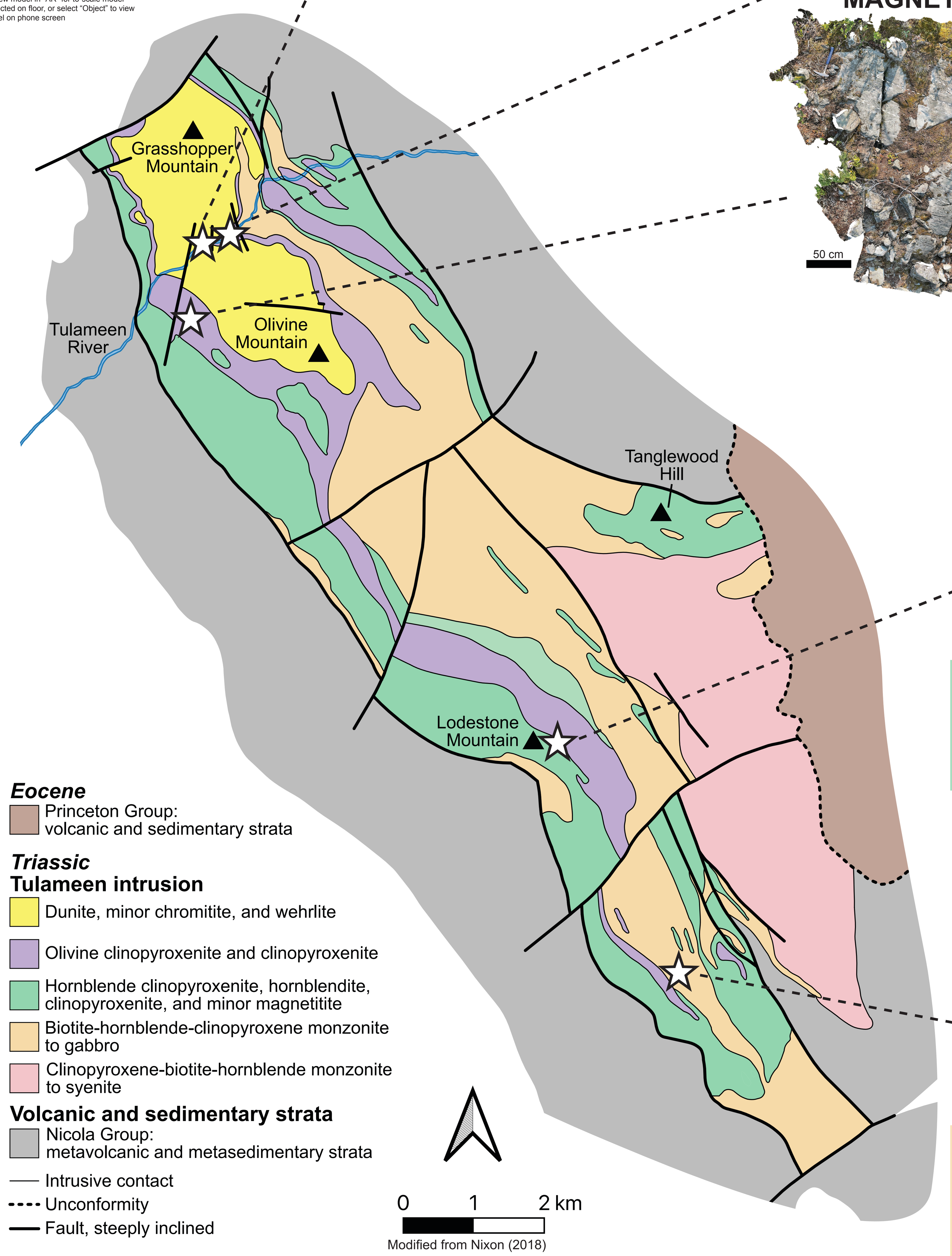

MAGNETITITE AND CLINOPYROXENE LAMINATIONS

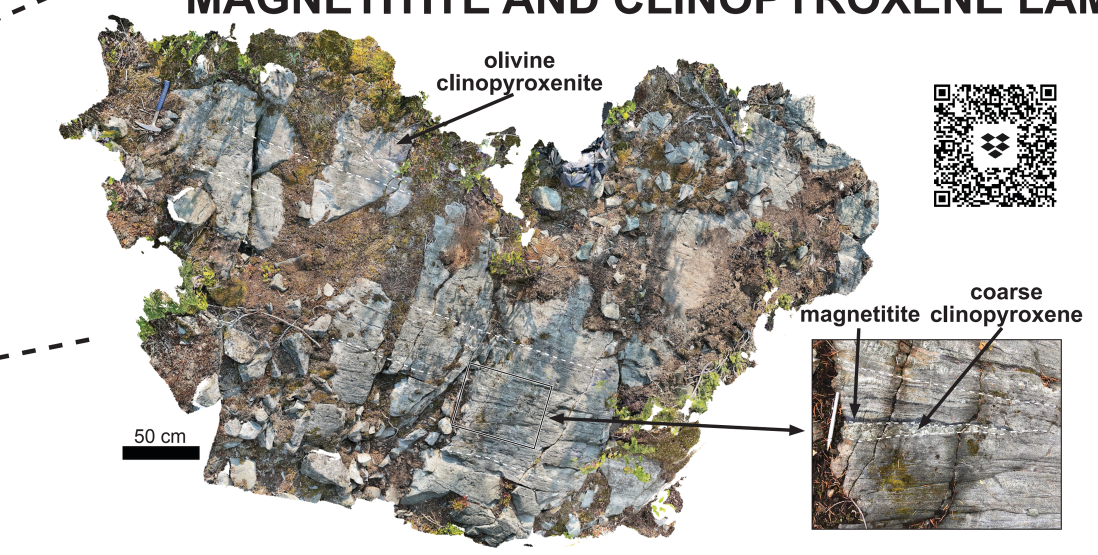

LEFT: 3D LiDAR model of outcrop containing laminated to layered outcrop of olivine-magnetite clinopyroxenite, magnetite clinopyroxenite, clinopyroxenite, and magnetitite. Layers, illustrated with dashed lines, are largely discontinuous and thicknesses pinch-and-swell.

RIGHT: Close-up photograph of outcrop showing discontinuous lamination of magnetitite and discontinuous layer of coarse clinopyroxenite within finely laminated olivine-magnetite clinopyroxenite. Scratcher for scale.

PEGMATITIC HORNBLENDITE AND HORNBLENDE LAMINATIONS

LEFT: 3D LiDAR model of hornblende clinopyroxenite with laminations (dashed lines) defined by the alignment of hornblende, cross-cut by pegmatitic hornblendite. Solid line shows contact.

TOP RIGHT: Photograph of hornblende clinopyroxenite boulder showing hornblende-defined laminations. Multiple layering directions (1,2) imply there was more than one intrusive event. Scratcher for scale.

BOTTOM RIGHT: Close-up photograph of 3D LiDAR model showing sharp contact between laminated hornblende clinoyroxenite and pegmatitic hornblendite. Scratcher for scale.

INTERMINGLED GABBRO-SYENITE AND HORNBLENDITE

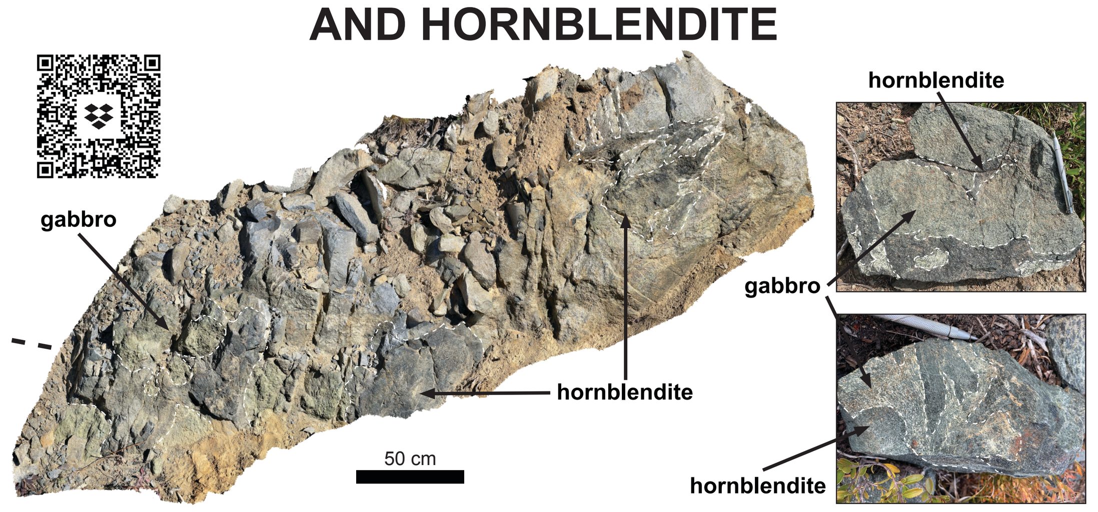

LEFT: 3D LiDAR model of hornblendite intermingled with gabbro. "Gabbro" is a field-term used for any rock mineralogically between monzogabbro and syenite. Contacts (dashed lines) are commonly cuspate. No clear indication of intrusive order is present, suggesting both rock types interacted as crystal mushes.

TOP RIGHT: Close-up photograph of boulder with intermingled gabbro and hornblendite. Enclaves of gabbro are present in hornblendite and enclaves of hornblendite are present in gabbro. Scratcher for scale.

BOTTOM RIGHT: Close-up photograph of boulder with intermingled gabbro and hornblendite. Gabbro is commonly foliated near contacts with hornblendite. Scratcher for scale.

MINERALOGICAL TEXTURES

OLIVINE

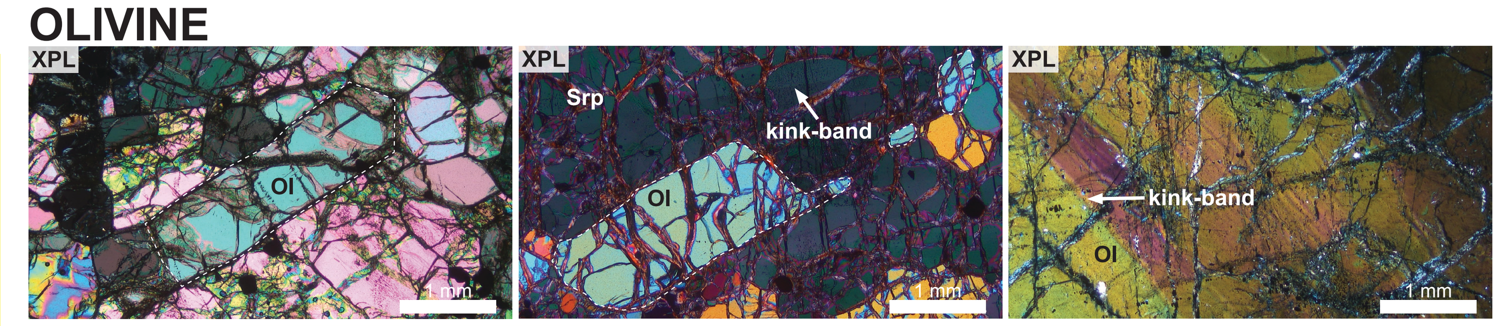

LEFT: Tabular, euhedral olivine crystal (dashed line) within dunite from Olivine Mountain.
CENTER: Tabular, euhedral olivine crystal (dashed line) intergrown with coarse, kink-banded olivine crystal within dunite from Olivine Mountain. The tabular crystal is not kink-banded suggesting there were at least two events leading to olivine crystallization.
RIGHT: Close-up of megacrystic olivine crystal (>1.5 cm) from dunite along the Tulameen River. This crystal is much coarser than host olivine within the sample, and intensely kink-banded, suggesting it was entrained.
ABBREVIATIONS: Chr = chromite, Cpx = clinopyroxene, Hbl = hornblende, Mag = magnetite, Ol = olivine, PPL = plane-polarized light, Srp = serpentine, TL = transmitted light, XPL = cross-polarized light.

CLINOPYROXENE

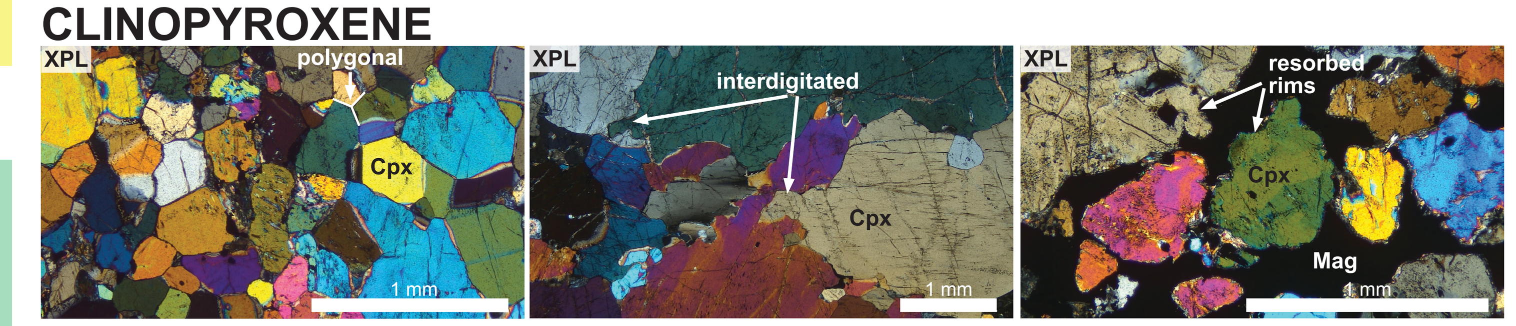

LEFT: Clinopyroxene crystals within olivine-bearing clinopyroxenite from the west-central part of the intrusion showing polygonal grain boundaries. Cumulus crystals re-equilibrated during cooling in the cumulate pile.
CENTER: Clinopyroxene grains within olivine clinopyroxenite from the Tulameen River showing interdigitated (consertal) grain boundaries. This texture suggests clinopyroxene did not grow in free space and then accumulate, but instead competed for space during crystallization.
RIGHT: Clinopyroxene crystals enclosed in magnetite within layered olivine-magnetite clinopyroxenite from the northwest part of the intrusion. Clinopyroxene crystals have been resorbed, implying they were not in equilibrium with their surroundings at magnetite saturation.

HORNBLENDE

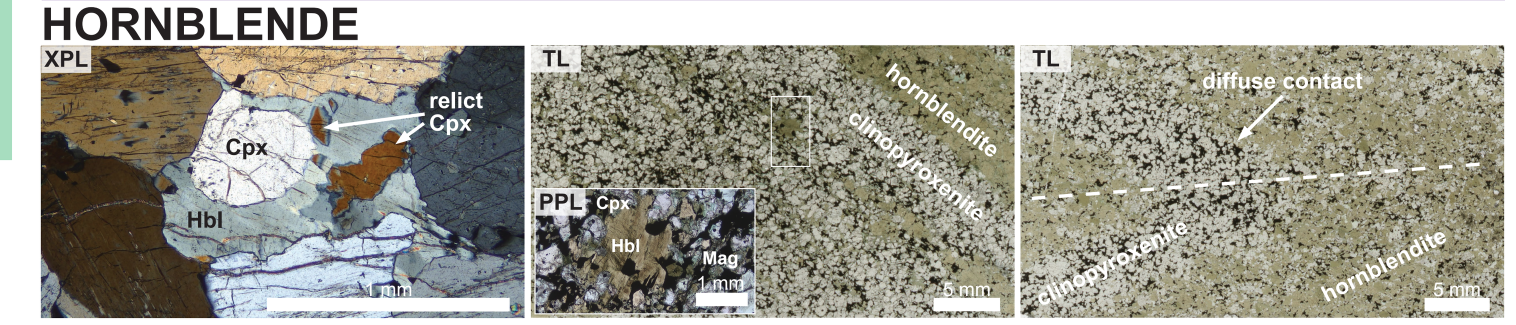

LEFT: Relict clinopyroxene crystals enclosed by hornblende within hornblende-olivine clinopyroxenite from the south part of the intrusion. This texture, along with blebby hornblende along clinopyroxene cleavage planes, is common in the Tulameen intrusion and evidence for clinopyroxene reaction with late-stage melts to produce hornblende (Nixon et al., in review).
CENTER: Magnetite-hornblende clinopyroxenite and hornblendite from the west-central part of the intrusion with irregular veins to laminations of hornblendite. Inset shows textural relationship between hornblende and clinopyroxene indicative of replacement.
RIGHT: Folded laminations to layers of magnetite clinopyroxenite and replacive magnetite-clinopyroxene hornblendite from northwest part of intrusion. Absence of foliation suggests that deformation occurred while the rock was still hot and mushy. Fold axial trace shown by dashed line.

MULTI-STAGE EMPLACEMENT

PHYSICAL MIXING?

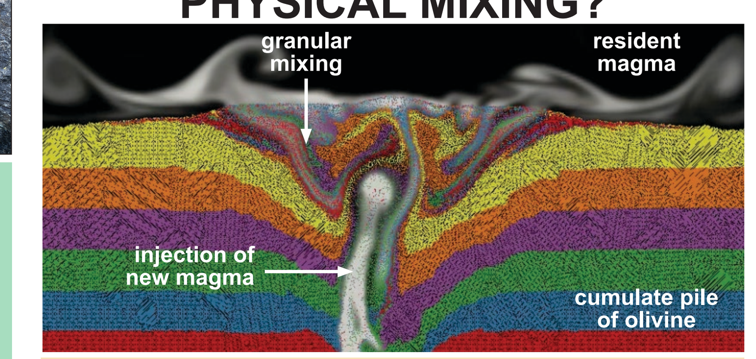

Diverse magmatic structures (e.g., discontinuous clinopyroxenite dikes, disaggregated dunite enclaves, discontinuous layering, intermingled gabbro and hornblendite) support a multiple-intrusive history where partially consolidated crystal mushes were physically mixed and remobilized by the injection of new magma pulses. The above numerical model (2.5 m wide, Bergantz et al., 2017) illustrates how this process may occur in an unconsolidated cumulate pile.

REACTION PROCESSES?

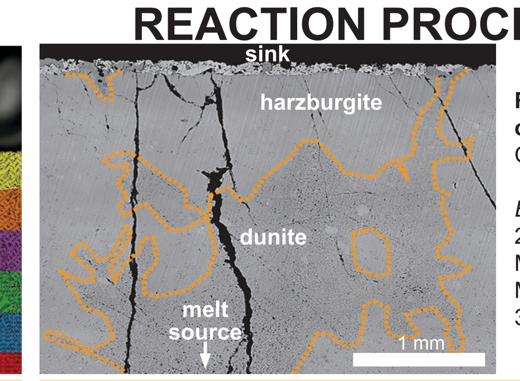

Reaction process in clinopyroxenite
Cpx + $Melt_1$ = Ol + $Melt_2$

Example:
$2CaMgSi_2O_6 + Melt_1 = Mg_2SiO_4 + Melt_2$, where $Melt_2 = Melt_1 + 2CaO + 3SiO_2$

Magmatic structures (e.g., hornblendite laminations/veins, dunite dike-like bodies) and mineral textures (e.g., replacive hornblende, resorbed clinopyroxene, interdigitated grains) suggest crystallization may have occurred as the product of melt-rock reaction. As an example (see reflected light image above), dunite dike-like bodies can be explained as the product of olivine crystallization from the reaction of pyroxene with a percolating basaltic melt (experiment by Pec et al., 2021).

CONCLUSIONS

1) Rocks of the Tulameen Alaskan-type ultramafic-mafic intrusion exhibit a wide range of magmatic structures and mineralogical textures.
2) Complex magmatic structures in the Tulameen intrusion are consistent with remobilization of crystal-rich magmas as the result of magmatic reinjection.
3) Mineral replacement occurred in the Tulameen intrusion as percolating and newly injected melts reacted with unconsolidated crystal mushes.

ACKNOWLEDGEMENTS

We thank Andrea Sanlorenzo for assistance in the field and Henry Crawford for discussions regarding iPhone LiDAR capabilities and helpful advice in operating the RPAS and processing imagery. The senior author is grateful for salary assistance from a University of British Columbia Four Year Doctoral Fellowship. Funding for this project is provided by a NSERC Discovery Grant to James Scoates and a grant from the Targeted Geoscience Initiative (TGI). We thank Megan Harris with the Upper Similkameen Indian Band (USIB) for providing archeological polygons for the field area and instructions for identifying archeological artifacts including lithics and modified trees.

Recommended Citation: Spence, D.W., Scoates, J.S., Goan, I.R., Nott, J.A., Nixon, G.T., and Milidragovic, D., 2024. Dynamic magmatic processes recorded in the Tulameen ultramafic-mafic Alaskan-type intrusion from outcrop-scale structures and mineral-scale textures. British Columbia Ministry of Energy, Mines and Low Carbon Innovation, British Columbia Geological Survey GeoFile 2024-14 (poster).

Bergantz, G.W., Schleicher, J.M., Burgisser, A., 2017, On the kinematics and dynamics of crystal-rich systems. Journal of Geophysical Research: Solid Earth 122, 6131–6159. **Colpron**, M., Nelson, J.L, 2011, A digital atlas of terranes for the northern Cordillera: Yukon Geological Survey, www.geolog.gov.yk.ca/bedrock_terrane.html. **Himmelberg**, G.R., Loney, R.A., 1995, Characteristics and petrogenesis of Alaskan-type ultramafic-mafic intrusions, southeastern Alaska. U.S. Geological Survey Professional Paper 1564. **Le Maitre**, R.W., 1989, A classification of igneous rocks and glossary of terms. Oxford, Blackwell Scientific Publications. **Manor,** M.J., Scoates, J.S., Nixon, G.T., Ames, D.E., 2016, The Giant Mascot Ni-Cu-PGE deposit, British Columbia: Mineralized conduits in a convergent margin tectonic setting. Economic Geology 111, 57-87. **Nixon**, G.T., Hammack, J.L., Ash, C.H., Cabri, L.J., Case, G., et al., 1997, Geology and platinum-group-element mineralization of Alaskan-type ultramafic-mafic complexes in British Columbia. British Columbia Geological Survey, Bulletin 93. **Nixon**, G.T., Manor, M.J., Jackson-Brown, S., Scoates, J.S., Ames, D.E., 2015, Magmatic Ni-Cu-PGE sulphide deposits at convergent margins. In: Ames, D.E., and M.G. Houlé, M.G., (Eds.), Targeted Geoscience Initiative 4: Canadian Nickel-Copper-Platinum Group Elements-Chromium Ore Systems-Fertility, Pathfinders, New and Revised Models, Geological Survey of Canada, Open File 7856, 17-34. **Nixon**, G.T., 2018, Geology of the Tulameen Alaskan-type ultramafic-mafic intrusion, British Columbia. British Columbia Geological Survey Open File 2018-2, 1:20,000 scale. **Pec**, M., Holtzman, B.K., Zimmerman, M.E., Kohlstedt, D.L., 2020, Influence of Lithology on Reactive Melt Flow Channelization. Geochemistry, Geophysics, Geosystems 21.